may also play a role in late-onset and sporadic PD (Chung *et al.* 2004; Yao *et al.* 2004; LaVoie *et al.* 2005). Parkin-associated endothelin receptor-like receptor (Pael-R/GPR37) was identified as an intracellular substrate of parkin, which has a propensity to accumulate in an unfolded form in the endoplasmic reticulum (ER) (Imai *et al.* 2001). When over-expressed in cultured cells, Pael-R tends to become misfolded and insoluble, inducing ER stress, and ultimately leading to cell death. Parkin ubiquitinates and promotes the degradation of misfolded species of Pael-R, resulting in the suppression of ER stress-induced cell death. The finding that panneuronal expression of Pael-R in *Drosophila* causes progressive selective loss of dopaminergic neurons further strongly supports a pathogenetic role for Pael-R in AR-JP (Yang *et al.* 2003). However, none of parkin null mouse models demonstrates either alteration in gross brain morphology or dopaminergic neuronal loss except for a recent report by Rodriguez-Navarro *et al.* (Goldberg *et al.* 2003; Itier *et al.* 2003; Von Coelln *et al.* 2004b; Perez and Palmiter 2005; Rodriguez-Navarro *et al.* 2007). A number of α-synuclein transgenic (tg), DJ-1- or PINK1- null mice models have also been created (Fernagut and Chesselet 2004; Goldberg *et al.* 2005; Kim *et al.* 2005). Although each of these models reproduces some of the pathological features of PD, obvious degeneration of dopaminergic neurons is not observed. The apparent preservation of dopaminergic neurons in these genetically modified animals suggests that obvious dopaminergic neuronal death may occur over a more protracted time scale than the average life spans of experimental animals, or that additional pathogenic event(s) may be required to induce such cell death.

Given that RNA interference (RNAi)-mediated down-regulation of endogenous *parkin* enhances the neurodegeneration of Pael-R tg *Drosophila* (Yang *et al.* 2003), deletion of the parkin gene in Pael-R tg mice may enhance the accumulation of Pael-R, resulting in neuronal degeneration. To test this hypothesis, we generated parkin-deficient/Pael-R-over-expressing double-mutant mice by crossbreeding parkin knockout (ko) mice with Pael-R tg mice. Here we show that *parkin*-ko/*Pael-R*-tg double-mutant mice exhibit early and progressive loss of dopaminergic neurons without formation of inclusion bodies, recapitulating the pathological characteristics of AR-JP. We provide compelling *in vivo* evidence of a mechanism linking progressive neuronal degeneration with persistent chronic ER stress. We also report that *parkin*-ko/*Pael-R*-tg double-mutant mice exhibit down-regulation of Ndufs4 and Ndufa10, two phosphorylated subunits of mitochondrial complex I, resulting in decrease in activity of mitochondrial complex I, suggesting that impairment of complex I activity might be the common pathway involved in various forms of PD including AR-JP. Moreover, the dopamine up-regulation caused by Pael-R over-expression seems to enhance oxidative stress, contributing to selective dopaminergic neuronal death.

Materials and methods

Generation of double-mutant mice over-expressing human Pael-R on a parkin null background

Transgenic mice that express human Pael-R under the control of the murine prion (PrP) or platelet-derived growth factor (PDGF) promoter (Imai *et al.* 2007) as well as the exon 3-deleted parkin null mice (Kitao *et al.* 2007) were produced as described. Double-mutant mice were generated by crossbreeding these two existing mouse lines. In the first step, parkin ko mice were bred to heterozygous Pael-R transgenic mice. Double-heterozygous mice generated in the first round of breeding were once more crossed with parkin ko mice to generate heterozygous Pael-R transgenic mice on a parkin null background (*parkin*-ko/non-tg or *parkin*-ko/*Pael-R*-het-tg). The *parkin*-ko/PrP- or PDGF-*Pael-R*-hetero-tg were cross-bred with each other to generate parkin null mice without Pael-R transgene (*parkin*-ko/*Pael-R*-non-tg), heterozygous or homozygous Pael-R transgenic mice lacking parkin (*parkin*-ko/PrP- or PDGF-*Pael-R*-het-tg and *parkin*-ko/PrP- or PDGF-*Pael-R*-homo-tg, respectively). In two successive breeding steps, cohorts of littermates with or without endogenous parkin expression and with or without transgenic Pael-R expression were generated in ratios consistent with Mendelian principles. Age-matched littermate mice were used in all experiments. All procedures involving animals conformed to the guidelines of the Institutional Animal Care Committee of RIKEN BSI and Kyoto University Graduate School of Medicine.

Immunohistochemistry

Mice were injected with pentobarbital (100 mg/kg; Sigma, St Louis, MO, USA) and perfused transcardially with ice-cold phosphate-buffered saline (PBS, pH 7.4), followed by 4% paraformaldehyde in PBS. Serial coronal sections at 16-μm thickness were collected on slides. Using standard avidin–biotin peroxidase method (Elite standard kit SK6100; Vector Laboratories, Burlingame, CA, USA), deparaffinized sections were stained with primary antibodies against tyrosine hydroxylase (TH, Chemicon, Temecula, CA, USA), α-synuclein (BD Transduction Laboratories, Lexington, KY, USA), BiP (Stressgen, Collegeville, PA, USA), CHOP (Santa Cruz Biotechnology, Santa Cruz, CA, USA) and ubiquitin (Dako, Carpinteria, CA, USA). For co-localization of TH with BiP or CHOP, deparaffinized sections were doubly stained with TH and BiP or CHOP, followed by reaction with Alexa 488- and 546-conjugated secondary antibodies (Molecular Probes, Eugene, OR, USA), and then examined with a LSM 510 confocal laser-scanning microscope (Carl Zeiss, Inc., Minneapolis, MN, USA).

Stereological analysis

Total numbers of TH-positive or Nissl-positive neurons in SNpc and locus coeruleus (LC) were determined using an unbiased optical fractionator method (Stereoinvestigator, MicroBrightField) as previously described (West 1993; Goldberg *et al.* 2003; Von Coelln *et al.* 2004b).

Behavioral tests

The mouse cohort for behavioral tests comprised 20 *parkin*-ko/*Pael-R*-non-tg mice, *parkin*-ko/PrP-*Pael-R*-het-tg mice and *parkin*-ko/PrP-*Pael-R*-homo-tg mice each. All tests were carried out by investigators blinded to the genotype of the animals being tested.

Western blot

Immunolabeling was performed using primary antibodies against α-synuclein (BD Transduction Laboratories), Pael-R (Imai *et al.* 2001), PKR-like ER-resident kinase (PERK, Santa Cruz), XBP1 (Santa Cruz), BiP (BD Transduction Laboratories), caspase-12 (Oncogene, Cambridge, MA, USA) JNK1/2 (Santa Cruz), phospho-JNK1/2 (Santa Cruz), CHOP (BioLegend, San Diego, CA, USA), TH (Chemicon), dopamine transporter (Chemicon), and vesicular monoamine transporter 2 (VMAT2, Chemicon), as well as horseradish peroxidase-conjugated secondary antibodies and ECL solutions (Amersham Pharmacia Biotech, Piscataway, NJ, USA). For densitometric analysis, images were scanned and densitometry was performed using the NIH IMAGE 1.4 software (Scion Corporation, Frederick, MD, USA).

RNA extraction and real-time PCR

Total RNA was isolated from freshly dissected midbrains using TRIzol Reagent (Invitrogen, Carlsbad, CA, USA) and first strand cDNA was synthesized from 2 μg of total RNA using SuperScript™ II Rnase H⁻ Reverse Transcriptase (Invitrogen) according to the manufacturer's instructions. Real-time PCR analysis was performed in triplicate on the ABI prism 7000 sequence detection system (Applied Biosystems, Foster City, CA, USA) using the SYBR Green PCR Master mix (Applied Biosystems). Results of real-time PCR were normalized against those for actin and plotted as ratio versus *parkin*-ko/*Pael-R*-non-tg.

Mitochondrial preparation and complex I, II–III, and IV activity assays

The mitochondrial complexes I, II–III, and IV activity assays were performed in triplicate on isolated mitochondria preparations as previously described (Hsu *et al.* 2005). The mitochondrial complexes and complex I subunits were detected using Total OXPHOS Complexes Detection Kit (MitoScience, Eugene, OR, USA), anti-8 kDa subunit monoclonal antibody (MitoScience), anti-18 kDa subunit monoclonal antibody (MitoScience) and anti-42 kDa subunit polyclonal antibody (Biocompare). Anti-COXIV monoclonal antibody (Molecular Probes) and anti-porin monoclonal antibody (Calbiochem, San Diego, CA, USA) were used as loading controls.

Measurement of catecholamines (HPLC)

To determine the concentration of catecholamines in striatal tissues by HPLC with electrochemical detection, male mice ($n = 12$ each) were decapitated, striata were dissected. The tissue was weighed and sonicated in 0.5 ml of ice-cold 0.1 M perchloric acid, to which 3, 4-dihydroxybenzylamine (DHBA) (Sigma) was added as the internal standard. DA and metabolites were detected with series coulometric detector (ESA, Inc., Chelmsford, MA, USA). Data were collected and processed on a CHROMELEON™ Chromatography Data Systems 6.40 (Dionex, Sunnyvale, CA, USA).

Protein carbonyl assay

Brain homogenate was assayed for protein carbonyls according to the manufacturer's instructions (OxyBlot™ Protein Oxidation Detection Kit, Chemicon).

Statistics

All values are presented as the mean ± SEM. Results were tested for significance using one-way ANOVA, followed by the Bonferoni *post hoc* test (SPSS 15.0 software). A significance level of $p < 0.05$ was used.

Results

Generation of *parkin*-ko/*Pael-R*-tg double-mutant mice

Transgenic mice over-expressing human Pael-R driven by murine PrP or PDGF promoter, designated PrP-*Pael-R* tg or PDGF-*Pael-R* tg mice, respectively, were generated as previously shown (Imai *et al.* 2007). PrP-*Pael-R* tg mice exhibited mild but significant loss of dopaminergic neurons (Fig. 1a). Neurodegeneration was not observed in PDGF-*Pael-R* tg mice even at the age of 2 years (Fig. 1b), probably due to relatively low expression level of Pael-R (Imai *et al.* 2007). Two lines of PrP- and PDGF-*Pael-R* tg mice were bred with parkin null mice (Kitao *et al.* 2007) to generate parkin null without Pael-R transgene (*parkin*-ko/*Pael-R*-non-tg), parkin null with Pael-R heterozygous tg (*parkin*-ko/PrP- or PDGF-*Pael-R*-het-tg) and Pael-R homozygous tg (*parkin*-ko/PrP- or PDGF-*Pael-R*-homo-tg) mice. We confirmed that 26-month-old *parkin*-ko mice did not display dopaminergic cell loss as compared with wild-type mice (Fig. 1c). Pael-R tended to be more insoluble in the midbrain region (Fig. S1), and throughout life the steady-state levels of both endogenous Pael-R and over-expressed human Pael-R remained unchanged (data not shown). Although parkin deletion had no effect on endogenous Pael-R monomer levels, both Triton X-100 soluble and insoluble fractions of over-expressed Pael-R monomer were significantly increased in *parkin*-ko/PrP-*Pael-R*-het-tg mice compared with PrP-*Pael-R*-het-tg mice with wild-type (wt) parkin (Fig. 1d and e). A higher molecular-weight band corresponding to the size of Pael-R dimer was constantly observed in all the samples (Fig. 1d). The high-molecular-weight bands were also observed in Pael-R null mice, indicating that they at least partially represent non-specific signals (Fig. 1f). However, given that non-specific signals are assumed to be almost identical between Pael-R null and wild-type mice, the decreased signal intensity in higher molecular-weight bands in Pael-R null mice compared with wt mice indicates that the higher molecular-weight bands in Pael-R expressing mice comprise both Pael-R dimer and the non-specific signals, and the former species are increased in the Triton X-100 insoluble fraction of parkin null mouse brains (Fig. 1d–f). Taken together, these data in Fig. 1(e) suggest that although less prominent than Pael-R transgene, insoluble species of endogenous Pael-R aggregates are likely to be increased in parkin null mice from 6 months of age.

Age-related neurodegeneration of dopaminergic neurons in *parkin*-ko/*Pael-R*-tg double-mutant mice

Progressive catecholaminergic neuronal loss was observed in both PrP-*Pael-R* and PGDF-*Pael-R* tg mice crossed with parkin null mice.

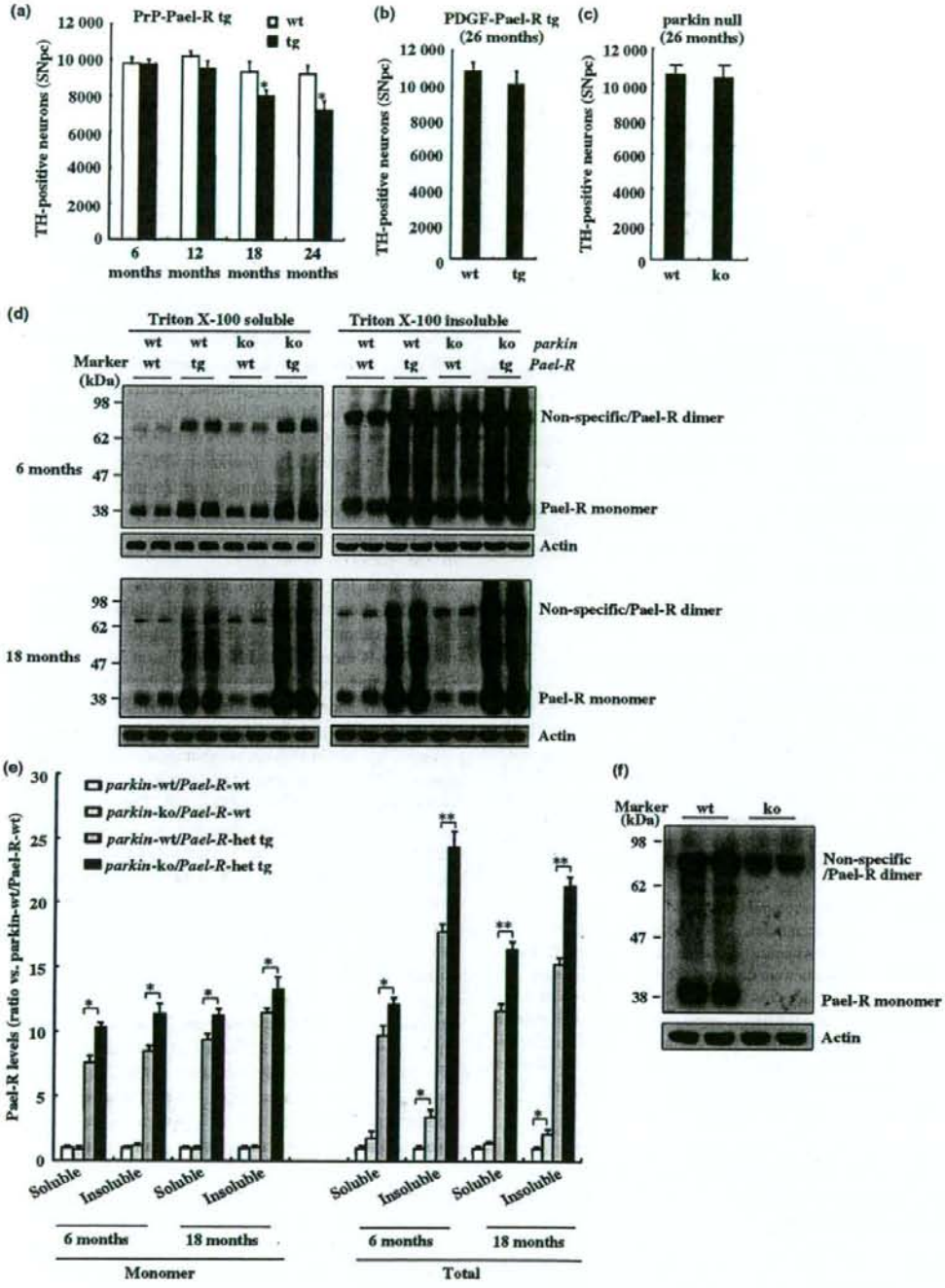

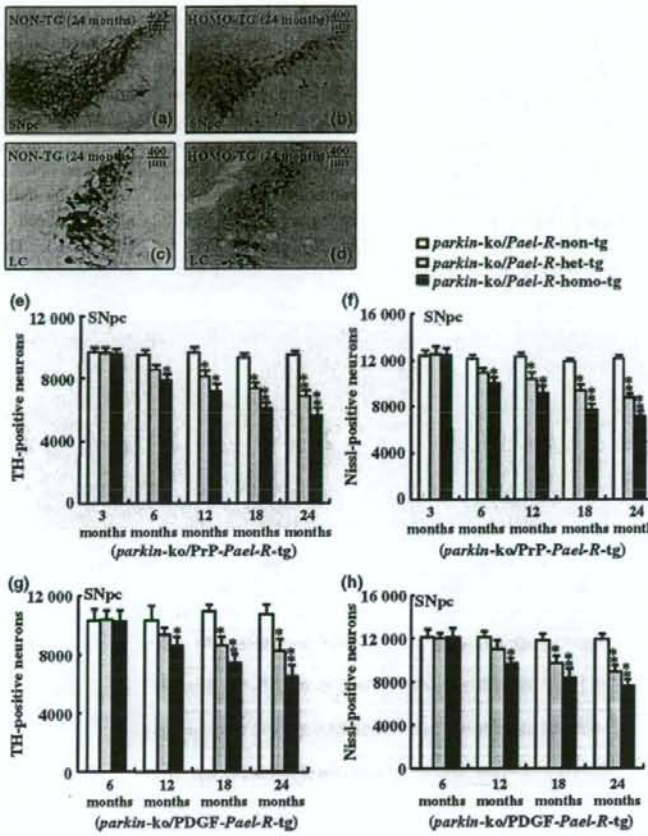

Fig. 2 Degeneration of TH-positive neurons in *parkin*-ko/PrP-*Pael-R*-tg double-mutant mice. (a and b) Representative photomicrographs of TH-immunoreactivity in SNpc of 24 months *parkin*-ko/*Pael-R*-non-tg and *parkin*-ko/PrP-*Pael-R*-homo-tg mice, respectively. (c and d) Representative photomicrographs of TH-immunoreactivity in LC of 24 months *parkin*-ko/*Pael-R*-non-tg and *parkin*-ko/PrP-*Pael-R*-homo-tg mice, respectively. (e and f), Number of TH-positive (e) or Nissl-positive neurons (f) in SNpc of *parkin*-ko/PrP-*Pael-R*-tg double-mutant mice. (g and h), Number of TH-positive (g) or Nissl-positive neurons (h) in SNpc of *parkin*-ko/PDGF-*Pael-R*-tg double-mutant mice. Data are expressed as mean ± SEM ($n = 10$). *, $p < 0.05$, **, $p < 0.01$ versus *parkin*-ko/*Pael-R*-non-tg.

Parkin-ko/PrP-*Pael-R*-tg mice exhibited decreased number of TH-positive neurons in the substantia nigra pars compacta (SNpc) and locus ceruleus (LC) regions compared with *parkin*-ko/*Pael-R*-non-tg mice (Fig. 2a–d). Unbiased stereological analyses revealed no difference in the number of TH-positive neurons in the SNpc of 3-month-old mice as assessed by either TH or Nissl staining. However, the number of TH-positive neurons exhibited age-dependent reduction beginning as early as 6 months in the *parkin*-ko/PrP-*Pael-R*-homo-tg double-mutant mice (Fig. 2e). The finding of similar loss of Nissl-positive neurons confirmed that the decrease of TH-positive neurons did not result from reduction of TH immunoreactivity, but from the loss of neurons *per se* (Fig. 2f). Similar loss of TH-positive neurons in the ventral tegmental area (VTA) and LC regions was also observed (Fig. S2a and b). Obvious loss of TH-positive

Fig. 1 Age-dependent loss of TH-positive neurons in Pael-R tg mice and absence of parkin increases steady-state levels of Pael-R. (a) Number of TH-positive neurons in Pael-R tg mice driven by PrP promoter. Values are the mean ± SEM ($n = 10$). *, $p < 0.05$, versus wild-type. (b) Number of TH-positive neurons in Pael-R tg mice driven by PDGF promoter ($n = 6$). (c) Number of TH-positive neurons in parkin ko mice ($n = 9$). (d) Representative western blot analysis of Triton X-100 soluble and insoluble lysates from midbrain of 6- and 18-month-old mice was performed using antibody recognizing both mouse and human Pael-R. The molecular weight was noted on the left. An antibody against actin was used as a loading control. (e) The expression levels of Pael-R (monomer, the band at approximately 38 kDa; total, the bands including Pael-R monomer, non-specific/Pael-R dimer, as well as smeared bands between Pael-R monomer and dimer) were quantified using optical density and normalized to that of actin. The protein levels are relative to those of parkin wt/Pael-R non-tg defined as 1. The data are presented as the mean ± SEM ($n = 6$). *, $p < 0.05$; **, $p < 0.01$. (f) Western blot analysis was performed on brain lysates from wt or Pael-R ko mice. The molecular weight was noted on the left.

neurons was observed at 18 months and 12 months in the PrP-Pael-R tg mice with and without parkin, respectively, indicating that loss of parkin predated the onset of neurodegeneration. The enhancement of Pael-R toxicity by parkin deficiency was more prominent in Pael-R tg mice driven by PDGF. Loss of TH-positive neurons became evident at 18 months of age in *parkin*-ko/PDGF-*Pael-R*-het-tg mice (Fig. 2g and h); whereas no frank neurodegeneration was observed in PDGF-*Pael-R*-het-tg mice expressing endogenous parkin even at 2 years of age (Fig. 1b). The number of hippocampal neurons in the dentate gyrus region, which also expressed high levels of Pael-R transgene (Fig. S1), was unaltered in *parkin*-ko/PrP-*Pael-R*-tg double-mutant mice (Fig. S3), suggesting that the cell loss occurred in catecholaminergic neuron-specific manner. Since *parkin*-ko/PrP-*Pael-R*-tg demonstrated more robust phenotype, we mainly analyzed *parkin*-ko/PrP-*Pael-R*-tg mice in the following analyses.

Tyrosine hydroxylase optical density in the striatum was also reduced in *parkin*-ko/PrP-*Pael-R*-homo-tg mice (Fig. 3a–c). This reduction in TH protein levels was confirmed by western blot at 18- and 24-month-old double-

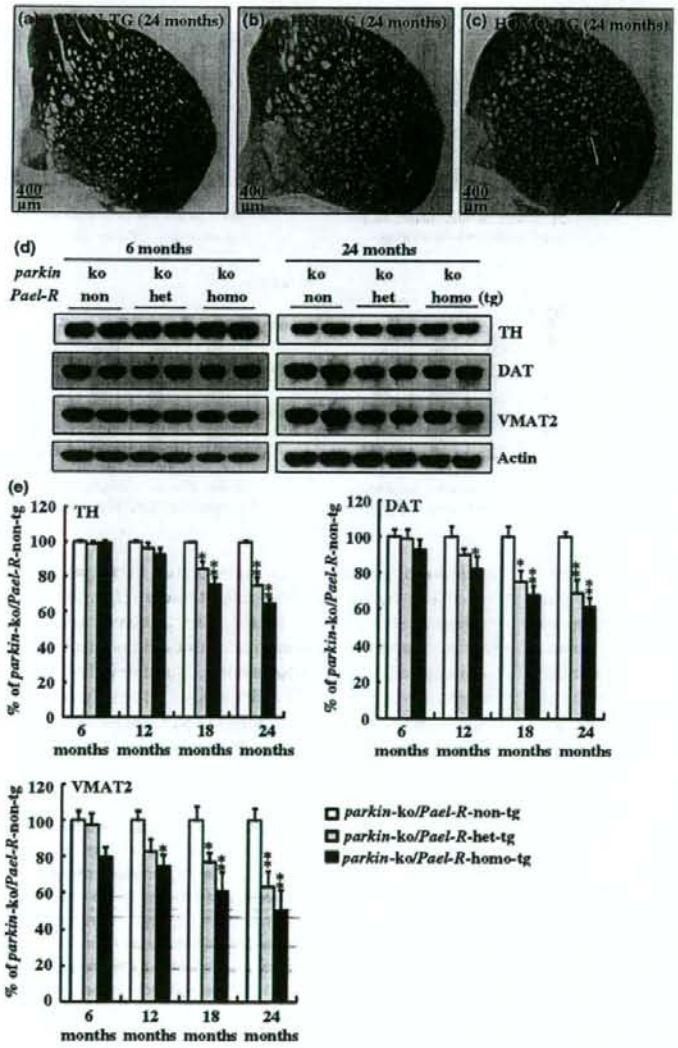

Fig. 3 Reduced TH-immunoreactivity in the striatum of *parkin*-ko/PrP-*Pael-R*-tg double-mutant mice. (a–c) Representative images of TH-immunoreactivity in the striatum of 24 months *parkin*-ko/*Pael-R*-non-tg, *parkin*-ko/PrP-*Pael-R*-het-tg and *parkin*-ko/PrP-*Pael-R*-homo-tg of mice, respectively. (d) Representative western blot images of TH, DAT and VMAT2 in young (6 M) and aged (24 M) mouse striatum. Actin was used as a loading control. (e) The expression levels of TH, DAT and VMAT2 (normalized to actin) were quantified using optical density. Data are expressed as mean ± SEM ($n = 6$). *, $p < 0.05$, **, $p < 0.01$ versus *parkin*-ko/*Pael-R*-non-tg.

mutant mice. Moreover, there were significant decreases in dopamine transporter and VMAT2 protein levels at these ages, consistent with the loss of dopaminergic nerve terminals (Fig. 3d and e).

No obvious behavioral defects in *parkin*-ko/PrP-*Pael-R*-tg double-mutant mice

Although observation of spontaneous, voluntary movements over 30 min in the open field test revealed that *parkin*-ko/PrP-*Pael-R*-tg mice tended to be more active at younger ages and less active at old ages compared with *parkin*-ko/*Pael-R*-non-tg mice, the difference failed to reach statistical significance (data not shown). In addition, these mice were similarly able to maintain their balance on the rotarod before falling off when young (data not shown). Although a tendency towards poor performance was observed in *parkin*-ko/PrP-*Pael-R*-tg mice at later stages, no significant difference was observed compared with *parkin*-ko/*Pael-R*-non-tg mice (data not shown).

Evidence for ER stress and activation of unfolded protein response in *parkin*-ko/PrP-*Pael-R*-tg double-mutant mice

We hypothesized that perturbation of ER homeostasis and triggering activation of unfolded protein response (UPR) underlies the progressive loss of dopaminergic neurons in *parkin*-ko/PrP-*Pael-R*-tg double-mutant mice. In the midbrain of *parkin*-ko/PrP-*Pael-R*-tg double-mutant mice, significant increase in BiP mRNA levels was clearly detected at the age of 6 months and maintained higher levels of transcription throughout life (Fig. 4a). On the other hand,

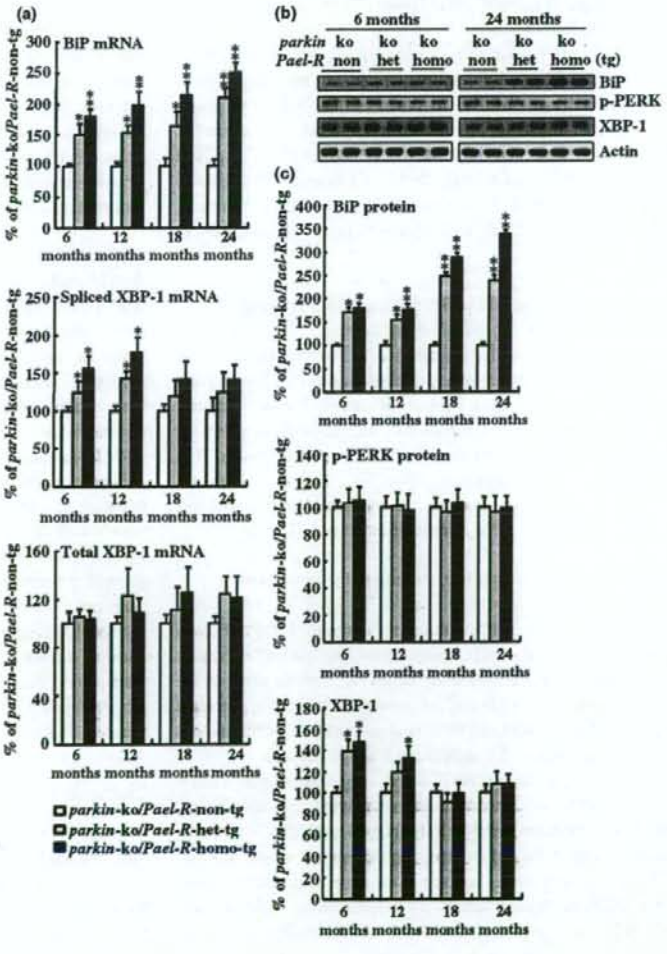

Fig. 4 Chronic and persistent activation of UPR in *parkin*-ko/*Pael-R*-tg double-mutant mice. (a) Real-time PCR was performed on mRNA extracted from the midbrain of *parkin*-ko/*Pael-R*-tg double-mutant mice. Data are expressed as mean ± SEM ($n = 6$). *, $p < 0.05$, **, $p < 0.01$ versus *parkin*-ko/*Pael-R*-non-tg. (b) Representative western blot images of BiP, phosphorylated form of PERK (p-PERK) and XBP-1 in the middle brain region of young (6 M) and aged (24 M) mice. Actin was used as a loading control. (c) The expression levels of BiP, p-PERK and XBP-1 protein (normalized to actin) were quantified using optical density. Data are expressed as mean ± SEM ($n = 6$). *, $p < 0.05$, **, $p < 0.01$ versus *parkin*-ko/*Pael-R*-non-tg.

the spliced form of XBP1 mRNA produced by 26-nucleotide splicing from primary XBP1 mRNA via the ribonuclease activity of IRE1 was increased only in early stages (Fig. 4a). Correspondingly, levels of BiP protein persistently increased in *parkin*-ko/PrP-*Pael-R*-tg double-mutant mice, whereas levels of XBP-1 increased only in the early stages (Fig. 4b and c). Collectively, these findings suggest that the IRE1 and ATF6 pathway of the UPR is activated in response to Pael-R accumulation *in vivo*.

On the other hand, PERK phosphorylation was unaltered at all time points examined (Fig. 4b and c), suggesting that global translational suppression induced by PERK phosphorylation may be transient in *parkin*-ko/*Pael-R*-tg double-mutant mice.

Evidence for ER-stress-mediated cell death: activation of JNK2, caspase-12 and CHOP/GADD153 in *parkin*-ko/*Pael*-R-tg double-mutant mice

Levels of CHOP were already substantially higher in *parkin*-ko/PrP-*Pael-R*-tg double-mutant mice at 6 months of age, followed by a nearly identical pattern of expression throughout life (Fig. 5a). The mRNA levels of caspase-12 and JNK2 were also increased at 12 months (Fig. 5a). The increase in levels of CHOP, JNK2 and caspase-12 mRNAs were accompanied by up-regulation of CHOP protein, phosphorylated JNK2 and cleaved form of caspase-12 (Fig. 5b and c).

Specific activation of UPR in dopaminergic neurons in *parkin*-ko/*Pael*-R-tg double-mutant mice

To confirm the specific occurrence of ER stress in dopaminergic neurons of the SNpc, double staining of TH and BiP or CHOP was performed. Up-regulation of BiP was restricted to TH-positive neurons and almost all TH-positive neurons exhibited intense expression of BiP in aged *parkin*-ko/PrP-*Pael-R*-tg double-mutant mice (Fig. S4a). Intense expression of CHOP was also observed in dopaminergic neurons in *parkin*-ko/PrP-*Pael-R*-tg double-mutant mice (Fig. S4b).

Evidence for impairment of complex I in *parkin*-ko/*Pael*-R-tg double-mutant mice

An approximately 30% reduction in complex I activity was observed in mitochondria isolated from *parkin*-ko/PrP-*Pael-R*-tg double-mutant mouse midbrain as well as the whole brain obtained from 18- and 24-month-old mice (Fig. 6a and data not shown), whereas there was no significant differences in complex II-III or IV activities (data not shown).

To investigate how Pael-R over-expression reduces complex I activity, we used a microarray approach to search for molecular markers and found that two transcripts, encoding Ndufs4 and Ndufa10, were significantly down-regulated. Consistent with the GeneChip data, semi-quantitative real time PCR confirmed decreased expression of Ndufs4 and Ndufa10 in *parkin*-ko/PrP-*Pael-R*-tg double-mutant mice when values were normalized to those for the house-keeping genes actin or 18S RNA (Fig. 6b). The reduction in expression of Ndufs4 (18 kDa) and Ndufa10 (42 kDa) proteins was confirmed by immunoblot analysis (Fig. 6c and d). We further used a mixture of monoclonal antibodies directed against various proteins in complexes of the electron transport chain to investigate the assembly of complex I in *parkin*-ko/PrP-*Pael-R*-tg mice. Quantitative band densitometry of western blot images revealed minor but significant reduction of protein from complex I, but not those from complexes II-V (Fig. 6c and d).

Abnormality of DA and its metabolites in *parkin*-ko/*Pael*-R-tg double-mutant mice

Striatal levels of DA were significantly increased in younger *parkin*-ko/PrP-*Pael-R*-het-tg and *parkin*-ko/PrP-*Pael-R*-homo-tg mice compared with age-matched *parkin*-ko/*Pael-R*-non-tg mice. Over time, however, the levels of DA in *parkin*-ko/PrP-*Pael-R*-tg double-mutant mice gradually decreased, and eventually significantly decreased at 24 months. Accordingly, the levels of 3, 4-dihydroxyphenylacetic acid (DOPAC) and homovanillic acid (HVA), the major metabolites of DA, were significantly increased in *parkin*-ko/PrP-*Pael-R*-homo-tg and *parkin*-ko/PrP-*Pael-R*-het-tg at younger stages (Fig. 7).

Evidence for oxidative damage in *parkin*-ko/*Pael*-R-tg double-mutant mice

It is widely believed that dopamine can induce neurotoxic effects via the formation of highly reactive oxygen species, quinones and semiquinones generated by dopamine auto-oxidation or via its enzymatic metabolism by MAO, leading to oxidative stress. The finding of increased levels of dopamine and its metabolites in *parkin*-ko/PrP-*Pael-R*-tg double-mutant mice therefore prompted us to investigate whether increased levels of oxidized proteins could be detected in these mice. Both *parkin*-ko/*Pael-R*-non-tg and *parkin*-ko/PrP-*Pael-R*-tg double-mutant mice represented age-dependent increases in levels of protein carbonyls, a general marker of oxidative damage. Levels of protein carbonyls were significantly higher in *parkin*-ko/PrP-*Pael-R*-tg double-mutant mice compared with *parkin*-ko/*Pael-R*-non-tg controls in the midbrain region (Fig. 8a), but not in the cortex region (Fig. 8b), suggesting that dopamine and/or its metabolites play important roles in the production of protein carbonyls.

Discussion

Recently, we have published a mouse model of PD by infecting Pael-R encoding adenovirus in the substantia nigra and shown that Pael-R over-expression *in vivo* leads to ER stress-induced death of dopaminergic neurons over a couple of weeks (Kitao *et al.* 2007). To confirm the results in a

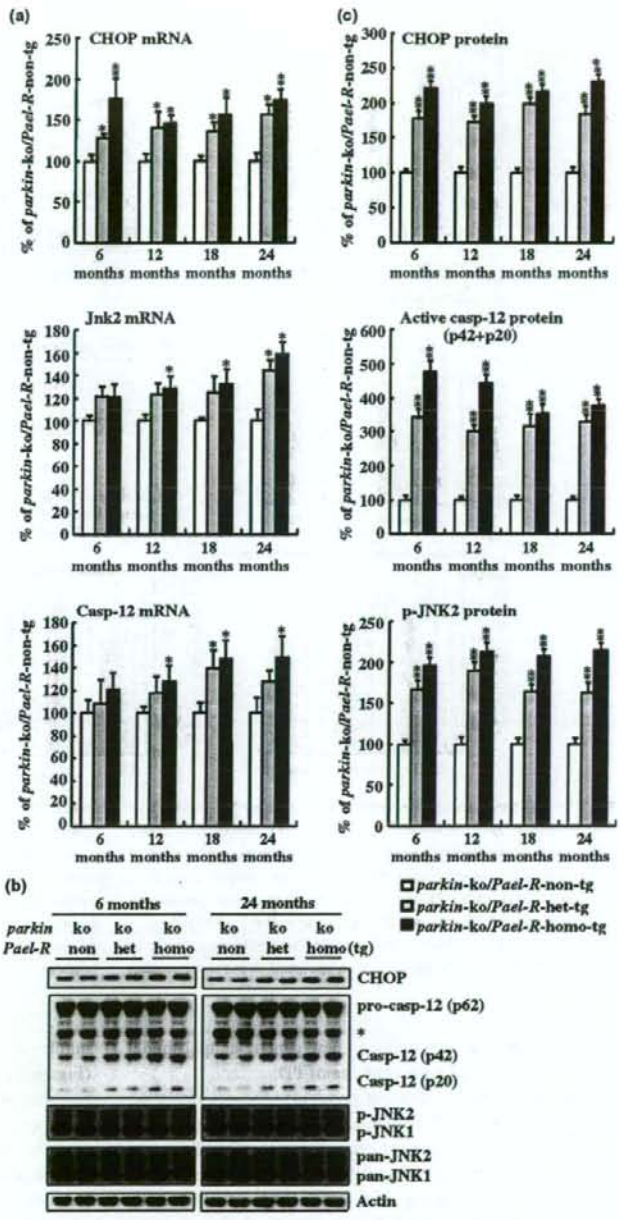

Fig. 5 Up-regulation of CHOP, JNK2 and caspase-12 in *parkin*-ko/PrP-*Pael-R*-het-tg and *parkin*-ko/PrP-*Pael-R*-homo-tg mice. (a) Real-time PCR was performed on the same samples as in Fig. 4a. Values were standardized to the level of actin mRNA and data are expressed as mean ± SEM ($n = 6$). *, $p < 0.05$, **, $p < 0.01$ versus *parkin*-ko/*Pael-R*-non-tg. (b) Representative western blot images of caspase-12 (Casp-12), CHOP, and phosphorylated form of JNKs (p-JNK1/2) in the midbrain region of young (6 M) and aged (24 M) mice. Actin was used as a loading control. The pan-JNK1/2 antibody was also used to assess the total amount of JNK proteins. The asterisk indicates a non-specific signal. (c) The expression levels of CHOP, p-JNK2 and active forms of caspase-12 (p42 and p20) (normalized to actin) were quantified using optical density. Data are expressed as mean ± SEM ($n = 6$). *, $p < 0.05$, **, $p < 0.01$ versus *parkin*-ko/*Pael-R*-non-tg.

genetic mouse model, we have generated *parkin*-ko/*Pael-R*-tg double-mutant mice, in which ER stress is evoked and selective and progressive catecholaminergic neuronal death without inclusion body formation occurs over 2 years, which recapitulates the main features of AR-JP. We obtained multiple lines of evidence indicating that chronic and persistent ER stress causes progressive loss of dopaminergic neurons over a long period of time in *parkin*-ko/*Pael-R*-tg

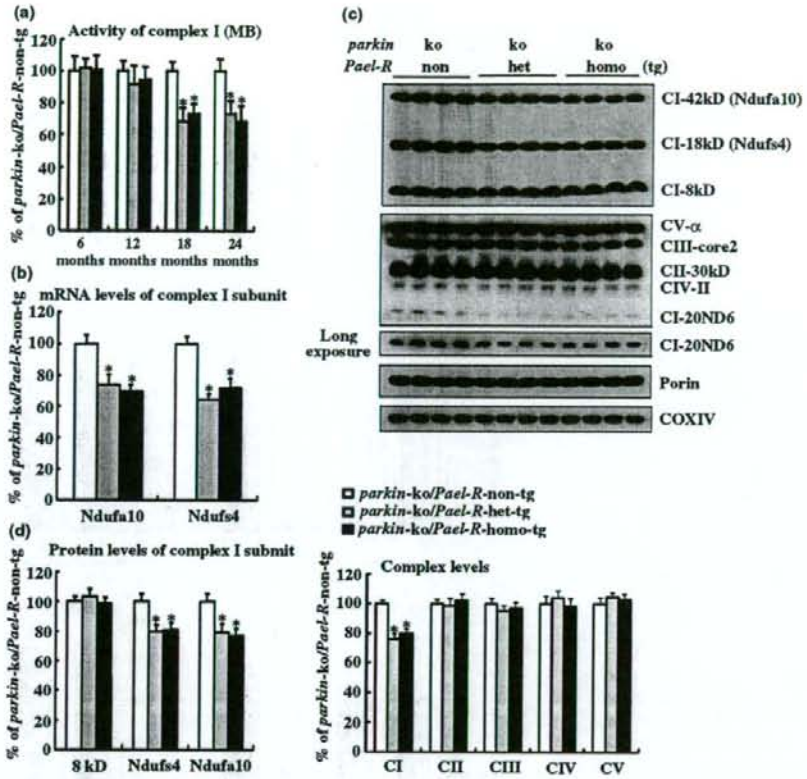

Fig. 6 Impaired mitochondrial complex I in *parkin*-ko/PrP-*Pael-R*-het-tg and *parkin*-ko/PrP-*Pael-R*-homo-tg mice. (a) Complex I activity analysis was performed on mitochondria isolated from *parkin*-ko/PrP-*Pael-R*-tg double-mutant mouse midbrains at later stages. Data are expressed as mean ± SEM ($n = 6$). *, $p < 0.05$ versus *parkin*-ko/*Pael-R*-non-tg. (b) Real-time PCR was performed on mRNA extracted from 18–24 months of *parkin*-ko/PrP-*Pael-R*-tg double-mutant mouse midbrains. The values were standardized to the level of actin mRNA and expressed as mean ± SEM ($n = 6$). *, $p < 0.05$ versus *parkin*-ko/*Pael-R*-non-tg. (c) Representative western blot images of subunits of complex I (Ndufa10, Ndufs4 and CI-8 kDa) and levels of complexes. Porin and COXIV were used as loading controls. (d) The expression levels of Ndufa10, Ndufs4, CI-8 kDa and complex I–V (normalized to COXIV) were quantified using optical density. Data are expressed as mean ± SEM ($n = 6$). *, $p < 0.05$ versus *parkin*-ko/*Pael-R*-non-tg.

double-mutant mice, providing a new genetic animal model to further explore the pathogenesis of PD.

In this study, parkin deletion promoted the accumulation of both soluble and insoluble Pael-R derived from the transgene, further supporting the idea that Pael-R is the substrate of parkin. Regarding the dopaminergic cell loss, it starts in PrP-*Pael-R*-het-tg mice at the age of 18 months, whereas it does in *Pael-R*-het -tg/*parkin*-ko double mutant mice at the age of 12 months (Figs 1a and 2e). Moreover, there were no difference in the dopaminergic cell number between 26-month-old PDGF-*Pael-R*-het-tg and wt mice, whereas 24-month-old PDGF-*Pael-R*-het-tg mice crossed with *parkin-ko* mice displayed reduced dopaminergic cell number compared with *parkin*-ko mice of the same age (Figs 1b, 2g and h). These data indicate that *parkin* deletion promotes neuronal loss by Pael-R accumulation.

Very recently, it was reported that around 35% TH-positive cell loss in the substantia nigra accompanied by motor behavioral abnormalities in foot print analysis occur in 24-month-old *parkin*-ko mice, raising the possibility that neurodegeneration phenotype of *parkin*-ko was simply added to that of Pael-R-tg mice(Rodriguez-Navarro *et al.* 2007). However, this is unlikely in our system, since 26-month-old *parkin*-ko mice displayed no dopaminergic neurodegeneration (Fig. 1c). The reasons for the discrepancies are unclear at this moment. Although we did not perform foot print

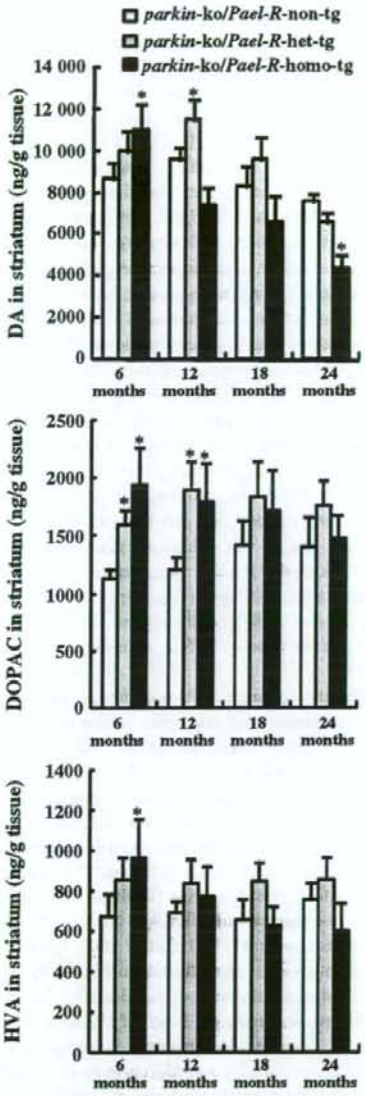

Fig. 7 HPLC analysis of DA and its metabolites in the striatum of *parkin*-ko/PrP-*Pael-R*-tg double-mutant mice. Data are expressed as mean ± SEM ($n = 12$). *, $p < 0.05$, **, $p < 0.01$ versus *parkin*-ko/*Pael-R*-non-tg.

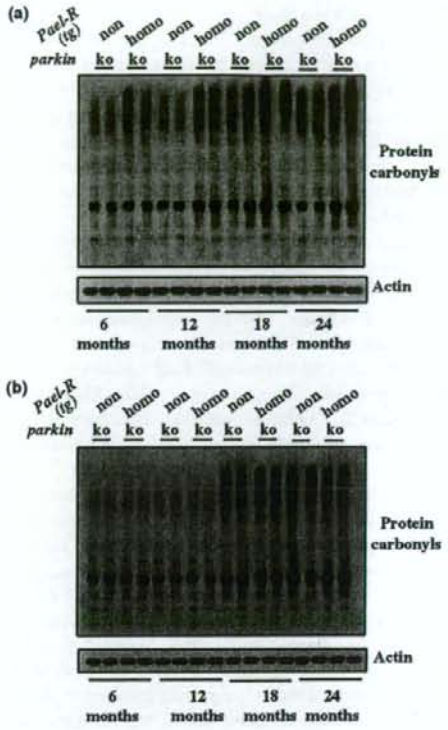

Fig. 8 Increased oxidative damage in *parkin*-ko/PrP-*Pael-R*-tg double-mutant mice. Carbonyl proteins were evaluated using lysates isolated from midbrain (a) and cortex (b). Incubation of the same blots with anti-actin antibody confirmed equivalent loading of proteins in each lane.

analyses, they might have detected abnormalities in *parkin*-ko/*Pael-R*-homo-tg double mutant mice which display 40% TH-positive cell loss at the age of 24 months.

Speculation regarding the involvement of ER stress in neuronal death has grown recently, due in part to reports of activation of the UPR in *in vitro* and *in vivo* models of neurodegenerative diseases (Nakagawa *et al.* 2000; Imai *et al.* 2001; Southwood *et al.* 2002; Takahashi and Imai 2003; Rao and Bredesen 2004; Tessitore *et al.* 2004). BiP has been shown to accompany ER stress and to be anti-apoptotic, while the failure of cells to counteract ER stress initiates activation of multiple pathways that lead to apoptosis (Breckenridge *et al.* 2003). CHOP is a member of CCAAT/enhancer-binding protein family that is induced by ER stress and participates in ER stress-mediated apoptosis (Oyadomari and Mori 2004). Excessive ER stress can also activate caspase-12, which resides on the outside of ER membrane (Nakagawa *et al.* 2000). Moreover, it has been shown that the ER transmembrane kinase/nuclease IRE1 can activate the c-Jun N-terminal kinase (JNK) by recruiting TRAF2 in response to ER stress (Urano *et al.* 2000). The early and consistent up-regulation of BiP, accompanied by activation of caspase-12, CHOP and JNK2 in *parkin*-ko/PrP-

Pael-R-tg double-mutant mice might represent cellular efforts to relieve ER stress. Over time, however, the cellular mechanisms fail to correct the continuous protein-folding defects, eventually leading to activation of multiple ER stress-mediated apoptotic processes. The finding of lack of alteration of phosphorylation of PERK is interesting, and suggests that persistent UPR induced in *parkin*-ko/PrP-*Pael-R*-tg double-mutant mice is not identical to conventional acute UPR.

Chronic and mild ER stress is known to induce UPR which allows for adaptation, instead of apoptosis, although UPR is designed to facilitate both adaptation to stress and apoptosis. Kaufmann and his colleagues have recently reported that survival is favored during chronic stress as a result of the intrinsic instabilities of mRNAs and proteins that promote apoptosis (Rutkowski *et al.* 2006; Rutkowski and Kaufman 2007). Consistent with their data, the scale of BiP up-regulation of double mutant mice at 24 months of age was greater than that of CHOP (Figs 4b and 5b).

It has been reported by several groups that complex I is decreased in the substantia nigra, skeletal muscle and platelets of patients with PD. Moreover, complex I inhibitors such as 1-methyl-4-phenyl-1,2,2,6-tetrahydropyridine and rotenone have been shown to cause dopaminergic cell death (Mizuno *et al.* 1998; Betarbet *et al.* 2000; Schapira 2001; Dauer and Przedborski 2003). More recently, phosphatase and tensin homologue-induced kinase 1 (PINK1), a mitochondrial protein, and DJ-1, a protein involved in oxidative stress partly located at mitochondria, turned out to be the genes responsible for familial PD termed PARK6 and PARK7, respectively (Dawson and Dawson 2003; Miller *et al.* 2003; Shen and Cookson 2004; Valente *et al.* 2004). These findings strongly support the idea that mitochondrial dysfunction, especially complex I deficiency plays a crucial role in the pathogenesis of PD. In this study, we found that complex I activity was decreased in Pael-R over-expressing mice, suggesting an important link between ER stress and mitochondrial dysfunction, both of which are thought to be involved in the pathogenetic mechanisms underlying PD.

In *parkin*-ko/*Pael-R*-tg double-mutant mice, the decrease in complex I activity was ascribable to transcriptional down-regulation of Ndufs4 and Ndufa10 subunits. Although we examined whether tunicamycin, thapsigargin or Pael-R over-expression-induced UPR is responsible for the down-regulation of Ndufs4 and Ndufa10 in cultured cells, only negative results were obtained (data not shown). The mechanism underlying down-regulation of Ndufs4 and Ndufa10 subunits of complex I in Pael-R tg mice is thus still unknown.

It is worth noting that down-regulated subunits Ndufs4 and Ndufa10 in PrP-*Pael-R*-tg mice are two exclusively phosphorylated proteins among complex I subunits (Schulenberg *et al.* 2003, 2004; Smeitink *et al.* 2004). Phosphorylation of mitochondrial proteins is pivotal to the regulation of respiratory activity in cells, and to signaling pathways leading to apoptosis, as well as for other vital mitochondrial processes. Ndufs4 has been suggested to be involved in assembly of functional complex I (Scacco *et al.* 2003). In addition, cyclic AMP-dependent intracellular signal transduction via phosphorylation of Ndufs4 has been reported to regulate the activity of complex I (Papa *et al.* 2001; Smeitink *et al.* 2001). The functional consequences of Ndufa10 phosphorylation await further investigation but might affect the binding affinity to NADH and in turn regulate the amount of fully active complex I (Schulenberg *et al.* 2003). Ndufa10 has appeared late in mitochondrial evolution and has been referred to as a "mammalian-specific" subunit of complex I (Cardol *et al.* 2004), consistent with a more regulatory role for this phosphorylated protein. It should also be noted that the phosphorylation sequence of Ndufa10 is likely to be a casein kinase I-like consensus motif, giving rise to the possibility that PINK1 is responsible for its phosphorylation (Schilling *et al.* 2005). Moreover, recent studies indicated that PINK1 and Parkin function, at least in part, in the same pathway, with PINK1 functioning upstream of Parkin, based on the observations that PINK1 and Parkin deficient *Drosophila* exhibit the identical phenotype with male sterility, apoptotic muscle degeneration and defects in mitochondrial morphology (Clark *et al.* 2006; Park *et al.* 2006; Yang *et al.* 2006). In this regard, whether Ndufs4 and Ndufa10 are substrates of PINK1 is an important issue to be clarified.

One feature common to dopaminergic neurons is the constitutive synthesis of dopamine within their cytoplasm. This is potentially important, given that metabolism of dopamine gives rise to various molecules that can act as endogenous toxins. If not properly handled, cytoplasmic dopamine might provoke neuronal damage through the generation of reactive oxygen species and, therefore, through mechanisms of oxidative stress (Shen and Cookson 2004). It has been shown that dopamine facilitates the transition of non-toxic α-synuclein protofibrils to toxic fibrils present in Lewy bodies (Lee *et al.* 2001; Sulzer 2001). It has also been reported that covalent modification of Parkin by dopamine lead to substantial inhibition of its E3 activity (LaVoie *et al.* 2005). Moreover, reduced level of VMAT2, leading to increase of cytoplasmic dopamine, is shown to result in progressive nigrostriatal neurodegeneration in mice (Caudle *et al.* 2007). This suggests the possibility that inappropriate metabolism of dopamine or its signaling or both might contribute to the selective degeneration of dopaminergic neurons. Notably, panneuronal expression of Pael-R in *Drosophila* causes age-dependent selective degeneration of dopaminergic neurons, and knockdown of *parkin* exacerbates this phenotype (Yang *et al.* 2003). Moreover, we have recently found that Alpha-methyl-p-tyrosine (AMPT), a TH inhibitor, ameliorates dopaminergic cell death induced by infection of adenovirus encoding Pael-R, implicating the pathological role of dopamine and its metabolites (Kitao

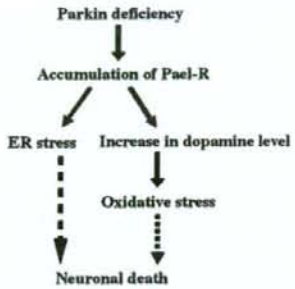

Fig. 9 The mechanisms underlying neuronal death in *parkin*-ko/PrP-*Pael-R*-tg double-mutant mice.

et al. 2007). *parkin*-ko/PrP-*Pael-R*-tg double-mutant mice demonstrate higher levels of DA, DOPAC and HVA early in the disease process and maintain higher levels of DOPAC and HVA throughout the lifetime. Correspondingly, these mice show higher levels of protein carbonyls, a well-known marker of oxidative damage specifically in the midbrain (Fig. 9). It is recently reported that oxidative stress compensatory mechanisms are impaired in 24-month-old *parkin* ko mice, suggesting that they may contribute to the increase of oxidative stress at the end-stage of double mutant mice(Rodriguez-Navarro *et al.* 2007).

Based on these observations, both chronic ER stress and excessive dopamine-mediated oxidative stress are likely to contribute to dopaminergic neuron-specific degeneration (Fig. 9). It is an intriguing question whether Pael-R is involved in the pathogenesis of sporadic PD, since Pael-R is localized to Lewy bodies(Murakami *et al.* 2004). The examination of Pael-R level accumulated in post-mortem brain of patients with sporadic PD will provide important clues to this question in the future. Taken together, *parkin*-ko/*Pael-R*-tg double-mutant mice provide an excellent opportunity to dissect the molecular mechanisms underlying AR-JP as well as other degenerative diseases caused by chronic ER stress.

Acknowledgments

This work was supported by the Grant-in aid from the Ministry of Health and Labour, Grant-in-Aid for Scientific Research on Priority Areas (Research on Pathomechanisms of Brain Disorders) from the MEXT of Japan to R.T. (18023020), Grant-in-Aid for Scientific Research to R.T. (18390255) from JSPS, Research Grant to R.T. from Takeda Science Foundation, Research Grant from RIKEN BSI to R.T., Grant-in-Aid for Young Scientists from the MEXT of Japan to H.-Q.W. (18700351).

Supporting information

Additional supporting information may be found in the online version of this article.

Fig. S1 Expression of Pael-R in distinct regions of brain.

Fig. S2 Loss of TH-positive neurons in *parkin-ko/PrP-Pael-R-tg* double-mutant mice.

Fig. S3 No reduction of Nissl-positive neurons in 24 months *parkin-ko/PrP-Pael-R-tg* double-mutant mice in the dentate gyrus region of hippocampus.

Fig. S4 Specific activation of UPR in *parkin*-ko/PrP-*Pael-R*-tg mice.

Please note: Blackwell Publishing is not responsible for the content or functionality of any supporting materials supplied by the authors. Any queries (other than missing material) should be directed to the corresponding author for the article.

References

Betarbet R., Sherer T. B., MacKenzie G., Garcia-Osuna M., Panov A. V. and Greenamyre J. T. (2000) Chronic systemic pesticide exposure reproduces features of Parkinson's disease. *Nat. Neurosci.* **3**, 1301–1306.

Breckenridge D. G., Germain M., Mathai J. P., Nguyen M. and Shore G. C. (2003) Regulation of apoptosis by endoplasmic reticulum pathways. *Oncogene* **22**, 8608–8618.

Cardol P., Vanrobaeys F., Devreese B., Van Beeumen J., Matagne R. F. and Remacle C. (2004) Higher plant-like subunit composition of mitochondrial complex I from Chlamydomonas reinhardtii: 31 conserved components among eukaryotes. *Biochim. Biophys. Acta* **1658**, 212–224.

Caudle W. M., Richardson J. R., Wang M. Z., Taylor T. N., Guillot T. S., McCormack A. L., Colebrooke R. E., Di Monte D. A., Emson P. C. and Miller G. W. (2007) Reduced vesicular storage of dopamine causes progressive nigrostriatal neurodegeneration. *J. Neurosci.* **27**, 8138–8148.

Chung K. K., Thomas B., Li X., Pletnikova O., Troncoso J. C., Marsh L., Dawson V. L. and Dawson T. M. (2004) S-nitrosylation of parkin regulates ubiquitination and compromises parkin's protective function. *Science* **304**, 1328–1331.

Clark I. E., Dodson M. W., Jiang C., Cao J. H., Huh J. R., Seol J. H., Yoo S. J., Hay B. A. and Guo M. (2006) Drosophila pink1 is required for mitochondrial function and interacts genetically with parkin. *Nature* **441**, 1162–1166.

von Coelln R., Dawson V. L. and Dawson T. M. (2004a) Parkin-associated Parkinson's disease. *Cell Tissue Res.* **318**, 175–184.

Dauer W. and Przedborski S. (2003) Parkinson's disease: mechanisms and models. *Neuron* **39**, 889–909.

Dawson T. M. and Dawson V. L. (2003) Molecular pathways of neurodegeneration in Parkinson's disease. *Science* **302**, 819–822.

Fernagut P. O. and Chesselet M. F. (2004) Alpha-synuclein and transgenic mouse models. *Neurobiol Dis* **17**, 123–130.

Goldberg M. S., Fleming S. M., Palacino J. J. *et al.* (2003) Parkin-deficient mice exhibit nigrostriatal deficits but not loss of dopaminergic neurons. *J. Biol. Chem.* **278**, 43628–43635.

Goldberg M. S., Pisani A., Haburcak M. *et al.* (2005) Nigrostriatal dopaminergic deficits and hypokinesia caused by inactivation of the familial Parkinsonism-linked gene DJ-1. *Neuron* **45**, 489–496.

Hsu M., Srinivas B., Kumar J., Subramanian R. and Andersen J. (2005) Glutathione depletion resulting in selective mitochondrial complex I inhibition in dopaminergic cells is via an NO-mediated pathway not involving peroxynitrite: implications for Parkinson's disease. *J. Neurochem.* **92**, 1091–1103.

Imai Y., Soda M. and Takahashi R. (2000) Parkin suppresses unfolded protein stress-induced cell death through its E3 ubiquitin-protein ligase activity. *J. Biol. Chem.* **275**, 35661–35664.

Imai Y., Soda M., Inoue H., Hattori N., Mizuno Y. and Takahashi R. (2001) An unfolded putative transmembrane polypeptide, which can lead to endoplasmic reticulum stress, is a substrate of Parkin. *Cell* **105**, 891–902.

Imai Y., Inoue H., Kataoka A. *et al.* (2007) Pael receptor is involved in dopamine metabolism in the nigrostriatal system. *Neurosci. Res.* **59**, 413–425.

Itier J. M., Ibanez P., Mena M. A. *et al.* (2003) Parkin gene inactivation alters behaviour and dopamine neurotransmission in the mouse. *Hum. Mol. Genet.* **12**, 2277–2291.

Kim R. H., Smith P. D., Aleyasin H. *et al.* (2005) Hypersensitivity of DJ-1-deficient mice to 1-methyl-4-phenyl-1,2,3,6-tetrahydropyridine (MPTP) and oxidative stress. *Proc. Natl Acad. Sci. USA* **102**, 5215–5220.

Kitada T., Asakawa S., Hattori N., Matsumine H., Yamamura Y., Minoshima S., Yokochi M., Mizuno Y. and Shimizu N. (1998) Mutations in the parkin gene cause autosomal recessive juvenile parkinsonism. *Nature* **392**, 605–608.

Kitao Y., Imai Y., Ozawa K. *et al.* (2007) Pael receptor induces death of dopaminergic neurons in the substantia nigra via endoplasmic reticulum stress and dopamine toxicity, which is enhanced under condition of parkin inactivation. *Hum. Mol. Genet.* **16**, 50–60.

LaVoie M. J., Ostaszewski B. L., Weihofen A., Schlossmacher M. G. and Selkoe D. J. (2005) Dopamine covalently modifies and functionally inactivates parkin. *Nat. Med.* **11**, 1214–1221.

Lee F. J., Liu F., Pristupa Z. B. and Niznik H. B. (2001) Direct binding and functional coupling of alpha-synuclein to the dopamine transporters accelerate dopamine-induced apoptosis. *FASEB J.* **15**, 916–926.

Lucking C. B., Durr A., Bonifati V. *et al.* (2000) Association between early-onset Parkinson's disease and mutations in the parkin gene. *N. Engl. J. Med.* **342**, 1560–1567.

Miller D. W., Ahmad R., Hague S. *et al.* (2003) L166P mutant DJ-1, causative for recessive Parkinson's disease, is degraded through the ubiquitin-proteasome system. *J. Biol. Chem.* **278**, 36588–36595.

Mizuno Y., Yoshino H., Ikebe S., Hattori N., Kobayashi T., Shimoda-Matsubayashi S., Matsumine H. and Kondo T. (1998) Mitochondrial dysfunction in Parkinson's disease. *Ann. Neurol.* **44**, S99–S109.

Murakami T., Shoji M., Imai Y., Inoue H., Kawarabayashi T., Matsubara E., Harigaya Y., Sasaki A., Takahashi R. and Abe K. (2004) Pael-R is accumulated in Lewy bodies of Parkinson's disease. *Ann. Neurol.* **55**, 439–442.

Nakagawa T., Zhu H., Morishima N., Li E., Xu J., Yankner B. A. and Yuan J. (2000) Caspase-12 mediates endoplasmic-reticulum-specific apoptosis and cytotoxicity by amyloid-beta. *Nature* **403**, 98–103.

Olanow C. W. and Tatton W. G. (1999) Etiology and pathogenesis of Parkinson's disease. *Annu. Rev. Neurosci.* **22**, 123–144.

Oyadomari S. and Mori M. (2004) Roles of CHOP/GADD153 in endoplasmic reticulum stress. *Cell Death Differ.* **11**, 381–389.

Papa S., Scacco S., Sardanelli A. M., Vergari R., Papa F., Budde S., van den Heuvel L. and Smeitink J. (2001) Mutation in the NDUFS4 gene of complex I abolishes cAMP-dependent activation of the complex in a child with fatal neurological syndrome. *FEBS Lett.* **489**, 259–262.

Park J., Lee S. B., Lee S. *et al.* (2006) Mitochondrial dysfunction in Drosophila PINK1 mutants is complemented by parkin. *Nature* **441**, 1157–1161.

Perez F. A. and Palmiter R. D. (2005) Parkin-deficient mice are not a robust model of parkinsonism. *Proc. Natl Acad. Sci. USA* **102**, 2174–2179.

Rao R. V. and Bredesen D. E. (2004) Misfolded proteins, endoplasmic reticulum stress and neurodegeneration. *Curr. Opin. Cell Biol.* **16**, 653–662.

Rodriguez-Navarro J. A., Casarejos M. J., Menendez J., Solano R. M., Rodal I., Gomez A., Yebenes J. G. and Mena M. A. (2007) Mortality, oxidative stress and tau accumulation during ageing in parkin null mice. *J. Neurochem.* **103**, 98–114.

Rutkowski D. T. and Kaufman R. J. (2007) That which does not kill me makes me stronger: adapting to chronic ER stress. *Trends Biochem. Sci.* **32**, 469–476.

Rutkowski D. T., Arnold S. M., Miller C. N., Wu J., Li J., Gunnison K. M., Mori K., Sadighi Akha A. A., Raden D. and Kaufman R. J. (2006) Adaptation to ER stress is mediated by differential stabilities of pro-survival and pro-apoptotic mRNAs and proteins. *PLoS Biol* **4**, e374.

Scacco S., Petruzzella V., Budde S., Vergari R., Tamborra R., Panelli D., van den Heuvel L. P., Smeitink J. A. and Papa S. (2003) Pathological mutations of the human NDUFS4 gene of the 18-kDa (AQDQ) subunit of complex I affect the expression of the protein and the assembly and function of the complex. *J. Biol. Chem.* **278**, 44161–44167.

Schapira A. H. (2001) Causes of neuronal death in Parkinson's disease. *Adv. Neurol.* **86**, 155–162.

Schilling B., Aggeler R., Schulenberg B., Murray J., Row R. H., Capaldi R. A. and Gibson B. W. (2005) Mass spectrometric identification of a novel phosphorylation site in subunit NDUFA10 of bovine mitochondrial complex I. *FEBS Lett.* **579**, 2485–2490.

Schulenberg B., Aggeler R., Beechem J. M., Capaldi R. A. and Patton W. F. (2003) Analysis of steady-state protein phosphorylation in mitochondria using a novel fluorescent phosphosensor dye. *J. Biol. Chem.* **278**, 27251–27255.

Schulenberg B., Goodman T. N., Aggeler R., Capaldi R. A. and Patton W. F. (2004) Characterization of dynamic and steady-state protein phosphorylation using a fluorescent phosphoprotein gel stain and mass spectrometry. *Electrophoresis* **25**, 2526–2532.

Shen J. and Cookson M. R. (2004) Mitochondria and dopamine: new insights into recessive parkinsonism. *Neuron* **43**, 301–304.

Shimura H., Hattori N., Kubo S. *et al.* (2000) Familial Parkinson disease gene product, parkin, is a ubiquitin-protein ligase. *Nat. Genet.* **25**, 302–305.

Smeitink J., Sengers R., Trijbels F. and van den Heuvel L. (2001) Human NADH:ubiquinone oxidoreductase. *J. Bioenerg. Biomembr.* **33**, 259–266.

Smeitink J. A., van den Heuvel L. W., Koopman W. J., Nijtmans L. G., Ugalde C. and Willems P. H. (2004) Cell biological consequences of mitochondrial NADH: ubiquinone oxidoreductase deficiency. *Curr. Neurovasc. Res.* **1**, 29–40.

Southwood C. M., Garbern J., Jiang W. and Gow A. (2002) The unfolded protein response modulates disease severity in Pelizaeus-Merzbacher disease. *Neuron* **36**, 585–596.

Sulzer D. (2001) alpha-synuclein and cytosolic dopamine: stabilizing a bad situation. *Nat. Med.* **7**, 1280–1282.

Takahashi R. and Imai Y. (2003) Pael receptor, endoplasmic reticulum stress, and Parkinson's disease. *J. Neurol.* **250**(Suppl. 3), III25–III29.

Tessitore A., del P. M. M., Sano R., Ma Y., Mann L., Ingrassia A., Laywell E. D., Steindler D. A., Hendershot L. M. and d'Azzo A. (2004) GM1-ganglioside-mediated activation of the unfolded protein response causes neuronal death in a neurodegenerative gangliosidosis. *Mol Cell* **15**, 753–766.

Urano F., Wang X., Bertolotti A., Zhang Y., Chung P., Harding H. P. and Ron D. (2000) Coupling of stress in the ER to activation of JNK protein kinases by transmembrane protein kinase IRE1. *Science* **287**, 664–666.

Valente E. M., Abou-Sleiman P. M., Caputo V. *et al.* (2004) Hereditary early-onset Parkinson's disease caused by mutations in PINK1. *Science* **304**, 1158–1160.

Von Coelln R., Thomas B., Savitt J. M., Lim K. L., Sasaki M., Hess E. J., Dawson V. L. and Dawson T. M. (2004b) Loss of locus coeruleus neurons and reduced startle in parkin null mice. *Proc. Natl Acad. Sci. USA* **101**, 10744–10749.

West M. J. (1993) New stereological methods for counting neurons. *Neurobiol. Aging* **14**, 275–285.

Yang Y., Nishimura I., Imai Y., Takahashi R. and Lu B. (2003) Parkin suppresses dopaminergic neuron-selective neurotoxicity induced by Pael-R in Drosophila. *Neuron* **37**, 911–924.

Yang Y., Gehrke S., Imai Y., Huang Z., Ouyang Y., Wang J. W., Yang L., Beal M. F., Vogel H. and Lu B. (2006) Mitochondrial pathology and muscle and dopaminergic neuron degeneration caused by inactivation of Drosophila Pink1 is rescued by Parkin. *Proc. Natl Acad. Sci. USA* **103**, 10793–10798.

Yao D., Gu Z., Nakamura T. *et al.* (2004) Nitrosative stress linked to sporadic Parkinson's disease: S-nitrosylation of parkin regulates its E3 ubiquitin ligase activity. *Proc. Natl Acad. Sci. USA* **101**, 10810–10814.

Oncogene (2008) 27, 6002–6011

www.nature.com/onc

ORIGINAL ARTICLE

Parkin as a tumor suppressor gene for hepatocellular carcinoma

M Fujiwara[1,5], H Marusawa[1], H-Q Wang[2,5], A Iwai[1], K Ikeuchi[1], Y Imai[3], A Kataoka[3], N Nukina[4], R Takahashi[2] and T Chiba[1]

[1]*Department of Gastroenterology and Hepatology, Graduate School of Medicine, Kyoto University, Kyoto, Japan;* [2]*Department of Neurology, Graduate School of Medicine, Kyoto University, Kyoto, Japan;* [3]*Laboratory for Motor System Neurodegeneration, RIKEN Brain Science Institute, Saitama, Japan and* [4]*Laboratory for Structural Neuropathology, RIKEN Brain Science Institute, Saitama, Japan*

The *parkin* was first identified as a gene implicated in autosomal recessive juvenile Parkinsonism. Deregulation of the *parkin* gene, however, has been observed in various human cancers, suggesting that the *parkin* gene may be important in tumorigenesis. To gain insight into the physiologic role of parkin, we generated *parkin*−/− mice lacking exon 3 of the *parkin* gene. We demonstrated here that *parkin*−/− mice had enhanced hepatocyte proliferation and developed macroscopic hepatic tumors with the characteristics of hepatocellular carcinoma. Microarray analyses revealed that *parkin* deficiency caused the alteration of gene expression profiles in the liver. Among them, endogenous *follistatin* is commonly upregulated in both nontumorous and tumorous liver tissues of *parkin*-deficient mice. *Parkin* deficiency resulted in suppression of caspase activation and rendered hepatocytes resistant to apoptosis in a follistatin-dependent manner. These results suggested that *parkin* deficiency caused enhanced hepatocyte proliferation and resistance to apoptosis, resulting in hepatic tumor development, partially through the upregulation of endogenous *follistatin*. The finding that *parkin*-deficient mice are susceptible to hepatocarcinogenesis provided the first evidence showing that *parkin* is indeed a tumor suppressor gene.
Oncogene (2008) **27**, 6002–6011; doi:10.1038/onc.2008.199; published online 23 June 2008

Keywords: *parkin*; hepatocellular carcinoma; follistatin

Introduction

The *parkin* was first identified as a gene implicated in autosomal recessive juvenile Parkinsonism (ARJP), the most frequent form of familial Parkinson disease (Farrer, 2006). Mutations in the *parkin* gene have been found among ARJP families worldwide (Kitada *et al.*, 1998). Parkin protein is characterized by a ubiquitin-like domain at the N terminus and two RING-finger motifs and in between RING-finger (IBR) motif at the C terminus (Kahle and Haass, 2004). There are an increasing number of studies, including ours, showing that parkin is an E3 ubiquitin ligase that targets a variety of candidate substrate proteins, resulting in proteosomal degradation (Jackson *et al.*, 2000; Shimura *et al.*, 2000; Takahashi *et al.*, 2003). Possible substrates for parkin include: *o*-glycosylated α-synphilin; α-synuclein interacting protein, synphilin-1 and Pael-R (Dawson and Dawson, 2003). These substrates suggest crucial roles for parkin in several cellular processes. However, the physiological role of parkin, especially in organs other than the brain, has not been clarified.

Human cancer develops through a multistep process involving the accumulation of genetic alterations that drive the progression of normal cells into malignant derivatives (Lengauer *et al.*, 1998). It has been shown that the development of human cancers can be triggered by various allelic deletions, which could theoretically contain tumor suppressor genes. Indeed, many tumors are associated with deletion of chromosomal regions containing the tumor suppressors *p53* and *Rb* (Hahn and Weinberg, 2002). One thing to be noted is that the loss of heterozygosity (LOH) within chromosomal region 6q25–q27 is frequently associated with various types of solid tumor, including carcinomas of the ovary (Saito *et al.*, 1996; Tibiletti *et al.*, 1996), breast (Rodriguez *et al.*, 2000), kidney (Morita *et al.*, 1991), lung (Kong *et al.*, 2000) and melanomas (Millikin *et al.*, 1991). On the other hand, the transfer of human chromosome 6 to melanoma cells resulted in the loss of their ability to form tumors in nude mice (Trent *et al.*, 1990). Moreover, normal chromosome 6 altered tumor growth properties *in vitro* and suppressed the tumorigenicity of breast cancer cells (Negrini *et al.*, 1994). These findings suggest that undefined genes present in chromosome 6 may play roles as tumor suppressor genes. Recently, physical mapping combined with LOH analysis identified *parkin* as a possible tumor suppressor gene, as the chromosomal region containing the highly

Correspondence: Dr H Marusawa, Department of Gastroenterology and Hepatology, Graduate School of Medicine, Kyoto University, 54 Kawara-cho, Shogoin, Sakyo-ku, Kyoto 606-8507, Japan.
E-mail: maru@kuhp.kyoto-u.ac.jp and Professor R Takahashi, Department of Neurology, Graduate School of Medicine, Kyoto University, 54 Kawara-cho, Shogoin, Sakyo-ku, Kyoto 606-8507, Japan.
E-mail: ryosuket@kuhp.kyoto-u.ac.jp
[5]These authors contributed equally to this work.
Received 4 December 2007; revised 9 April 2008; accepted 1 May 2008; published online 23 June 2008

unstable FRA6E common fragile site region at 6q25–q27 is frequently deleted in breast and ovarian tumors (Cesari *et al*., 2003; Denison *et al*., 2003). In addition, another study reported that 4 of 11 hepatocellular carcinoma (HCC) cell lines had heterozygous deletion of *parkin* exon, and that parkin protein expression was significantly decreased or absent in all 11 HCC cells (Wang *et al*., 2004). These findings suggest that *parkin* is important as a tumor suppressor and is involved in the development of human cancers. To gain insight into the physiological and pathological role of parkin, we generated *parkin*−/− mice and analysed their phenotypes.

Results

Development of hepatocellular carcinoma in parkin−/− mice

The mutant *parkin* allele lacking exon 3 was generated by homologous recombination in murine AK18.1 ES cells (129S4/SvJaeSor), and the *parkin* mutation was maintained in a mixed 129/C57BL6SJL (75/25) genetic background (Kitao *et al*., 2007). *Parkin*−/− mice were born alive and appeared healthy, but body weight was significantly reduced in both male and female *parkin*−/− mice compared to wild-type mice (31.77 ± 0.72 g for *parkin*−/− male mice vs 36.23 ± 0.58 g for wild-type male mice at 48 weeks of age; $n = 42$ for each; Figure 1a). *Parkin*−/− mice were neurologically normal with no obvious behavioral abnormalities, and no neuropathologic changes were observed in aged *parkin*−/− mice, which is consistent with recent reports (Goldberg *et al*., 2003; Itier *et al*., 2003; Palacino *et al*., 2004; Von Coelln *et al*., 2004; Perez and Palmiter, 2005). In contrast to the lack of neuropathologic abnormalities, a striking phenotypic change occurred in the livers of *parkin*−/− mice. Despite the low body weight of *parkin*−/− mice, their livers were enlarged: at 48 weeks of age, their liver weight was 1.5 times greater than that of wild-type mice (1.55 ± 0.24 vs 1.09 ± 0.34 g; Figure 1b). Thus, the ratio between liver weight and body weight of *parkin*−/− mice was about twofold greater than that of wild-type mice at 48 weeks of age.

The livers of aged *parkin*−/− mice had a distinct phenotype. In addition to hepatomegaly, macroscopic hepatic tumors developed in 33% (12/36) and 45% (19/42) of *parkin*−/− mice at 72 and 96 weeks of age, respectively. In contrast to the parkin−/− mice, no hepatic tumors were admitted in the wild-type and *parkin*+/− mice examined at the same age. Histological examination revealed that these tumors were trabecular-type liver cancers, which were similar to human HCC (Figure 2a). It is noteworthy that all HCC tissues examined expressed α-fetoprotein (AFP), the best known tumor marker for human HCC, whereas no AFP expression was observed in the nontumorous regions of either *parkin*−/− livers or wild-type livers (Figure 2b). Moreover, strong immunoreactivity for β-catenin was observed in HCC tissues of the *parkin*−/− mice, whereas staining for β-catenin was absent in the nontumorous region of the *parkin*-deficient liver (Figure 2c).

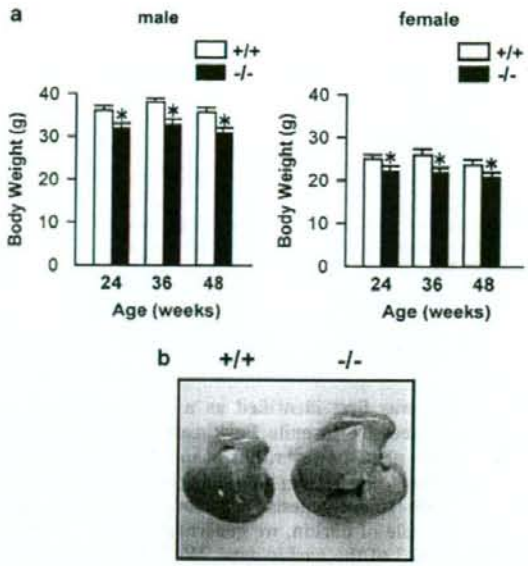

Figure 1 Enhanced proliferation of hepatocytes in the *parkin*-deficient liver. (**a**) Evolution of body weight for wild-type (+/+, open bars) and *parkin*-deficient (−/−, black bars) mice. **P*-value of <0.05 as determined by Student's *t*-test. (**b**) Liver anomalies in *parkin*−/− mice. Macroscopic hepatomegaly was observed in 48-week-old *parkin*−/− mice.

Gene expression profiles in nontumorous and tumorous liver tissues of parkin−/− mice

Consistent with previously reported *parkin*−/− mice models (Goldberg *et al*., 2003), immunoblot analyses revealed no significant changes in the expression levels of several parkin substrate proteins (data not shown). On the other hand, it has been demonstrated that parkin has a RING-IBR-RING motif, which has been predicted to be involved in the regulation of gene expression (Morett and Bork, 1999). To provide an insight into the molecular mechanism by which *parkin* deficiency contributes to hepatocarcinogenesis, we analysed gene expression profiles of nontumorous and tumorous liver tissues from *parkin*−/− mice using cDNA microarray analyses. Out of 43 800 genes analysed, we identified a number of genes that were upregulated or downregulated in the liver tissues of *parkin*−/− mice. Among them, the expression ratios of 302 genes (including 59 genes of unknown function) were greater than fivefold in the tumorous liver tissues compared to those in normal livers of wild-type mice (Supplementary Table 1). Similarly, we identified 96 genes (including 31 genes of unknown function) that were upregulated in nontumorous liver tissues of *parkin*−/− mice compared to liver tissues of wild-type

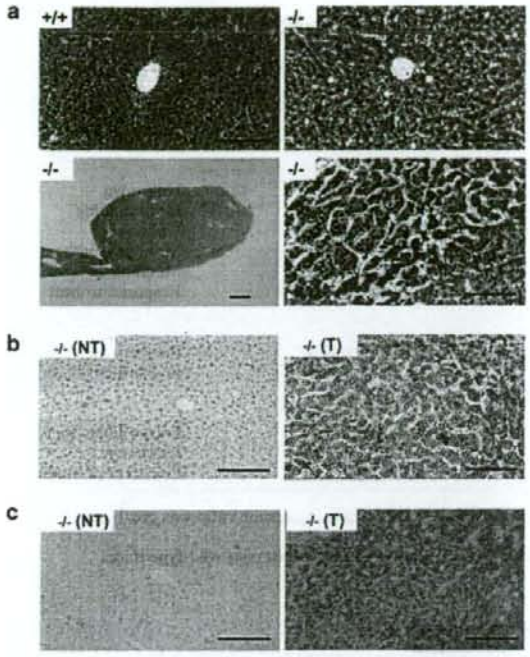

Figure 2 Development of hepatocellular carcinoma in *parkin*-deficient mice. (**a**) Histologic analyses of hepatic tumor specimens from *parkin*−/− mice obtained at 72 weeks of age. The upper panels show × 200 magnification of hematoxylin and eosin (HE)-stained liver sections of nontransgenic controls (+/+, left) and the nontumorous region of *parkin*-deficient mice (−/−, right). Scale bar = 200 μm. The lower panels show liver tumors of *parkin*−/− mice. Macroscopic view of representative hepatic tumor (left) and HE-stained section of the liver tumor (right; × 200) are shown. Scale bar = (left) 1 mm, (right) 200 μm. (**b**, **c**) Immunostaining for α-fetoprotein (AFP) and β-catenin in the hepatic tumor developed in *parkin*−/− mice. Immunohistochemical study for AFP (**b**) and β-catenin (**c**) protein was carried out in the nontumorous region (NT) and the tumor (T) of *parkin*−/− mice (magnification: × 200). Scale bar = 200 μm.

mice (Supplementary Table 2). To identify the key molecule responsible for enhanced hepatocyte proliferation, and thus hepatocarcinogenesis, in *parkin*−/− mice, we searched for genes that were commonly upregulated in both nontumorous and tumorous liver tissues of the *parkin*−/− mice. This ensured that the genes selected were not confined to nontumorous or to tumorous tissues. Using this filter, we identified 13 genes that were commonly upregulated in livers of *parkin*−/− mice (Table 1). These 13 upregulated genes included those expressing enzymes (cytochrome p450 (4a10), abhydrolase domain containing 1, hydroxysteroid dehydrogenase-4 and asparagine synthetase), molecules involved in metabolism, chemokine ligand 1 and the activin-antagonist, *follistatin*. The filter also identified genes that were downregulated in nontumorous (104 genes) and tumorous liver tissues (138 genes) of *parkin*−/− mice whose expression ratio was less than fivefold than those of corresponding genes in normal liver. Among them, 17 genes were commonly downregulated in both nontumorous and tumorous liver tissues of the *parkin*−/− mice (Supplementary Table 3), however, the role of these genes in tumorigenesis is unclear at present. The microarray data have been submitted to the Gene Expression Omnibus (GEO) public database at National Center for Biotechnology Information (NCBI) under the accession number GSE9651.

Upregulation of endogenous follistatin in parkin−/− *mice*

Follistatin is an endogenous antagonist of activin and controls proliferation, differentiation and apoptosis of numerous cell types in an autocrine and paracrine manner (Chen *et al*., 2002; Harrison *et al*., 2005). Recent studies demonstrated that overexpression of follistatin is associated with enhanced hepatocyte proliferation, resulting in enlargement of the liver *in vivo* (Kogure *et al*., 2000; Takabe *et al*., 2003). As *follistatin* expression is commonly upregulated in the livers of *parkin*−/− mice, we focused on the hepatic expression of follistatin to clarify the mechanism by which *parkin* deficiency causes HCC. To confirm the reliability of microarray data, we first examined the expression of *follistatin* using semiquantitative and quantitative real-time RT–PCR assays with primers specific for mouse *follistatin*. Expression of β-*actin* and *18S rRNA* transcripts served as internal controls. Although transcription of *follistatin* was low in the normal livers of wild-type mice, expression of *follistatin* was substantially upregulated in both tumorous and nontumorous liver tissues of *parkin*−/− mice (Figure 3a). Transcripts of the transforming growth factor-β superfamily genes in liver tissues, including the genes for *inhibin-A*, *inhibin-B*, *BMP2* and *BMP4*, were also examined, but there were no differences in their expression between wild-type and *parkin*−/− mice (Figure 3b). To further confirm the upregulation of *follistatin* expression in *parkin*−/− mice, we performed immunoblot analyses using antibodies specific for follistatin. The follistatin protein was not detected in lysates from liver tissues of wild-type mice. In contrast, follistatin protein was clearly detectable in the tumorous liver tissues of *parkin*−/− mice (Figure 3c), consistent with the data obtained from the quantitative real-time RT–PCR analyses. To examine the tissue-specific expression of *follistatin*, total RNA samples extracted from wild-type and *parkin*−/− mice tissues (liver, kidney, lung, small intestine and brain) were analysed using quantitative real-time RT–PCR. We found that *follistatin* mRNA was highly expressed in the livers of *parkin*−/− mice, whereas substantially lower levels of *follistatin* expression were observed in various tissues of the wild-type mice and in the liver of the *parkin*+/− mice (Figure 3d).

To determine whether parkin is involved in transcriptional regulation of *follistatin*, we examined the effect of *parkin* on expression of endogenous follistatin using cultured hepatoma-derived cells. First, we confirmed that follistatin protein expression was markedly decreased in Hep3B cells with parkin expression

Table 1 List of commonly upregulated genes in both nontumorous and tumorous liver tissues of *parkin*−/− mice

Gene name	*Tumor/nontumor*[a]	*Ref seq ID*	*Function*
Cell growth			
Chemokine ligand 1 (Cxcl1)	21.5/11.7	NM_008176	Angiogenesis
Follistatin (Fst)	10.7/8.0	NM_008046	Antagonist of activin
Biological process			
Asparagine synthetase (Asns)	92.4/39.2	NM_012055	Unknown
Apolipoprotein A-4 (Apoa4)	58.8/5.3	NM_007468	Lipid binding
Camello-like 4 (Cml4)	15.7/27.1	NM_023455	Unknown
Cytochrome p450 (4a10)	14.7/18.5	NM_177406	Monooxygenase
Sulfotransferase family 1E, member 1	6.36/14.4	NM_023135	Metabolism
Heat-shock protein 1A (Hspa1a)	5.63/5.07	NM_010479	Response to heat
Metabolism			
Hydroxysteroid dehydrogenase-4 (Hsd3b4)	8.29/29.1	NM_008249	Biosynthesis of steroids
Hydroxysteroid dehydrogenase-5 (Hsd3b5)	7.69/24.9	NM_008295	Biosynthesis of steroids
Cellular component			
WAP four-disulfide core domain 15	60.7/5.04	NM_138685	Extracellular space
Abhydrolase domain containing 1	8.65/14.7	NM_021304	Unknown
Serum amyloid P component	6.49/7.54	NM_011318	Precursor of amyloid

Genes that were upregulated in both nontumorous and tumorous liver tissues of *parkin*−/− mice whose expression ratio was greater than fivefold compared to normal livers of wild-type mice are shown.
[a]Values are fold increases in nontumorous and tumorous liver tissues of *parkin*−/− mice relative to normal livers of wild-type mice.

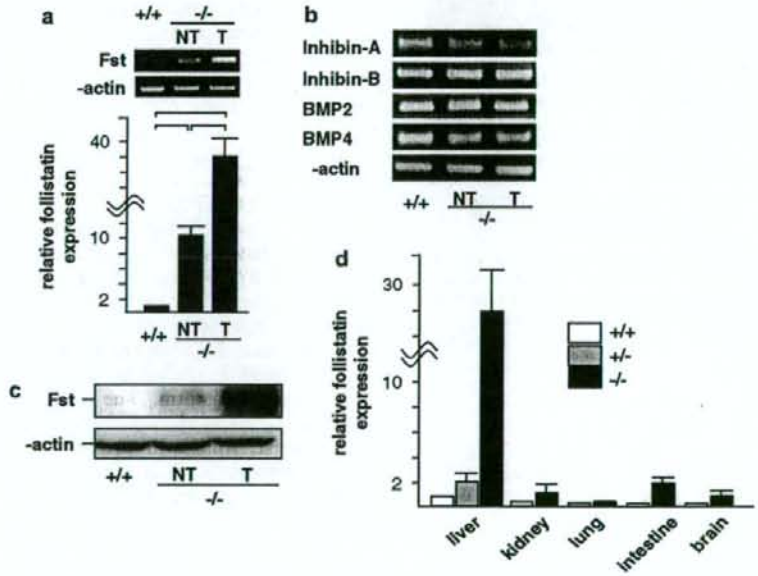

Figure 3 Upregulation of *follistatin* expression in the *parkin*-deficient liver. (**a**) Expression of endogenous *follistatin* (Fst, upper panel) or β-actin (lower panel) in the livers of wild-type (+/+), nontumorous (NT) and tumorous (T) tissues of *parkin*-deficient mice. The lower graphs show the relative mRNA levels of *follistatin* measured by quantitative real-time RT–PCR using *18S rRNA* as an internal control (mean ± s.d.; $n=3$). *P-value of <0.05 as determined by Student's t-test. (**b**) Total RNA was isolated from the liver tissues of wild-type (+/+), NT and T liver tissues of *parkin*−/− mice. RT–PCR was performed using 0.5 μg of each RNA as a template and oligonucleotide primer sets specific for mice *inhibin-A, inhibin-B, BMP2, BMP4* and *β-actin*. (**c**) Total protein was isolated, and immunoblot analyses were carried out using anti-Fst (upper panel) or anti-β-actin (lower panel) in the livers of wild-type (+/+), NT and T liver tissues of *parkin*−/− mice. (**d**) Expression levels of endogenous *follistatin* in various organs. Quantitative real-time RT–PCR was carried out using the total RNA isolated from the various organs of wild-type (+/+, open bars) and *parkin*−/− mice (black bars). The expression levels of Fst transcripts in the liver of the *parkin*+/− are also shown as a gray bar.

(Supplementary Figure 1a). Quantitative real-time RT–PCR analyses revealed that overexpression of *parkin* in cultured hepatoma-derived cells resulted in the substantial downregulation of *follistatin* expression, whereas mutant *parkin* lacking exons 3–4 had no significant effects on the expression of *follistatin*

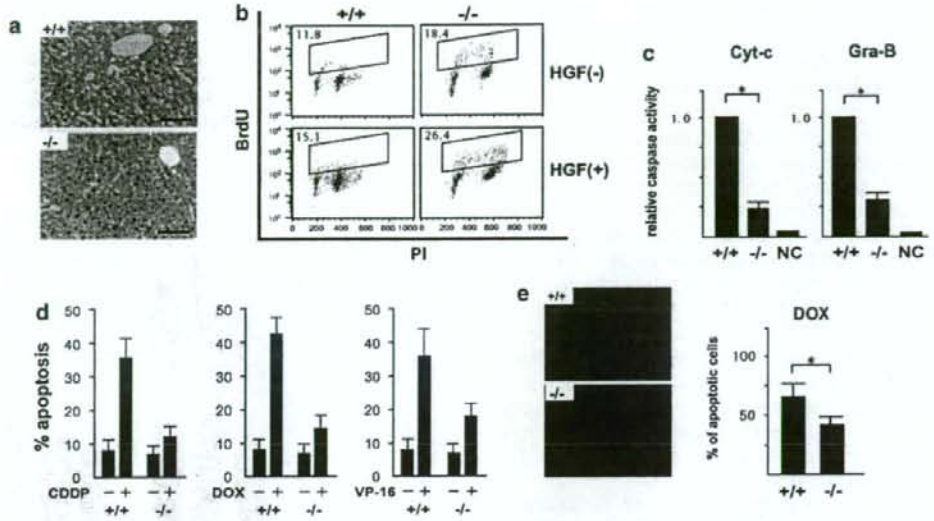

Figure 4 Increased cell proliferation and reduced apoptosis of hepatocytes of *parkin*−/− mice. (**a**) Increased proliferation of hepatocytes derived from the nontumorous region of *parkin*−/− mice. Hepatocyte proliferation in wild-type (+/+) and *parkin*-deficient (−/−) mice was evaluated by proliferating cell nuclear antigen (PCNA) staining. Scale bar = 200 μm. (**b**) 5-Bromodeoxyuridine (BrdU) labeling on the primary hepatocytes before and after the treatment with hepatocyte growth factor (HGF). Mouse primary hepatocytes were established from *parkin*−/− or wild-type (+/+) mice and cultured in fresh medium for 24 h, followed by the treatment with recombinant HGF (10 ng/ml) for 48 h. The levels of BrdU labeling were determined by flow cytometric analyses. (**c**) *Parkin* deficiency caused an overall inhibition of caspase activation induced by cytochrome *c* (Cyt-c) and granzyme B (Gra-B). Lysates were prepared from liver specimens of wild-type (+/+), *parkin*−/− mice and normalized for total protein content. Caspase activity was measured using the caspase-3 substrate, Ac-DEVD-pNA (10 mM), after the addition of Cyt-c and dATP (left graph) or Gra-B (right graph). Results are expressed relative to caspase activity generated in the normal liver of wild-type mice (mean ± s.d.; $n = 3$). Reaction mixture without Cyt-c or Gra-B was included as a negative control (NC). **P*-value of <0.05 as determined by Student's *t*-test. (**d**, **e**) *Parkin*−/− hepatocytes show resistance to apoptosis induced by various anticancer drugs. Primary hepatocytes were established from wild-type (+/+) or *parkin*−/− mice. Then, cells were treated for 48 h with 200 μM cisplatin (CDDP), 10 μM doxorubicin (DOX) or 400 nM etoposide (VP-16). Cell viability was determined by a trypan blue dye exclusion assay (**d**) and Annexin-V staining (**e**) (mean ± s.d.; $n = 3$). The percentage of apoptotic cells was determined from >200 cells, manually counted in triplicate. **P*-value of <0.05 as determined by Student's *t*-test.

(Supplementary Figure 1b). Moreover, expression of *parkin* in Huh7 cells resulted in dose-dependent reductions in the relative amounts of *follistatin* transcripts (Supplementary Figure 1c). Use of reporter plasmids encoding the promoter region of the *follistatin* gene revealed that parkin expression resulted in a substantial decrease in luciferase activity in the transfected cells (Supplementary Figure 1d). Finally, we investigated the expression profiles of *follistatin* as well as the *parkin* gene in clinical specimens of human HCC tissues. We found that most of the liver cancer specimens that lacked *parkin* expression showed upregulation of *follistatin* compared to the nontumorous region of the liver (Supplementary Figure 2a). In contrast, human HCC specimens that had a *parkin* expression level similar to the nontumorous regions did not show such enhanced expression of *follistatin* transcripts (Supplementary Figure 2b). Taken together, these findings indicate that the expression of *follistatin* was specifically elevated in the *parkin*-deficient livers and suggest that *parkin* is involved in the transcriptional regulation of *follistatin* expression in hepatocytes.

Parkin deficiency comprising follistatin upregulation renders hepatocytes more resistant to apoptosis

To investigate the molecular basis of hepatomegaly in *parkin*−/− mice, hepatocyte proliferation rate was determined using PCNA (proliferating cell nuclear antigen) labeling. Consistent with the development of hepatomegaly, enhanced hepatocyte proliferation was observed in the livers of 48-week-old *parkin*−/− mice (Figure 4a). Increased proliferation of *parkin*−/− hepatocytes was further supported by 5-bromodeoxyuridine (BrdU) labeling of primary hepatocytes, which showed that hepatocyte growth factor (HGF) stimulation resulted in a higher level of BrdU labeling in *parkin*−/− hepatocytes than in those of wild-type mice (Figure 4b). To clarify the functional significance of *follistatin* upregulation, we investigated whether *parkin*-deficient hepatocytes are resistant to apoptosis because of upregulation of *follistatin*. To determine whether caspase activation is suppressed in *parkin*-deficient hepatocytes, cytosolic extracts from the livers of *parkin*−/− and wild-type mice were prepared, normalized for total protein content and then treated with either cytochrome *c* or granzyme B. In control extracts

from wild-type mice, cytochrome *c* or granzyme B induced the activation of caspases, as measured by cleavage of the caspase substrate, Ac-DEVD-pNA. By comparison, far less caspase activity was induced by cytochrome *c* or granzyme B in extracts prepared from *parkin*−/− livers (Figure 4c). To investigate the anti-apoptotic features of *parkin*−/− hepatocytes, we established cultured primary hepatocytes from *parkin*−/− mice and compared levels of apoptosis induced by cisplatin (CDDP), doxorubicin (DOX) or etoposide (VP-16) between *parkin*−/− hepatocytes and wild-type cells. As shown in Figure 4d, significantly less cell death was induced by CDDP, DOX or VP-16 in the *parkin*−/− hepatocytes compared to the normal hepatocytes, consistent with the finding that *parkin* deficiency caused suppression of caspase activation. Annexin-V assay revealed significantly reduced numbers of apoptotic *parkin*−/− hepatocytes after treatment with DOX compared to those of the hepatocytes derived from the wild-type mice (Figure 4e).

To determine whether upregulation of *follistatin* is involved in reducing apoptosis in *parkin*−/− cells, we used small-interfering RNA (siRNA) to inhibit the expression of endogenous *follistatin* in primary mouse hepatocytes. Induction of *follistatin*-specific, but not control, double-strand synthetic RNAs reduced endogenous *follistatin* transcript levels in both normal and *parkin*−/− mouse hepatocytes, although only trace amounts of *follistatin* were detectable in hepatocytes derived from wild-type mice (Figure 5a). In the primary hepatocytes derived from *parkin*−/− mice, treatment with DOX was more effective in inducing apoptosis in hepatocytes treated with *follistatin* siRNA compared to those treated with control siRNA (Figure 5b). In contrast, a far less suppressive effect of knockdown of endogenous *follistatin* was observed on apoptosis of normal hepatocytes. These findings suggest that upregulation of *follistatin* is closely associated with suppression of caspase activation and apoptosis in *parkin*−/− hepatocytes.

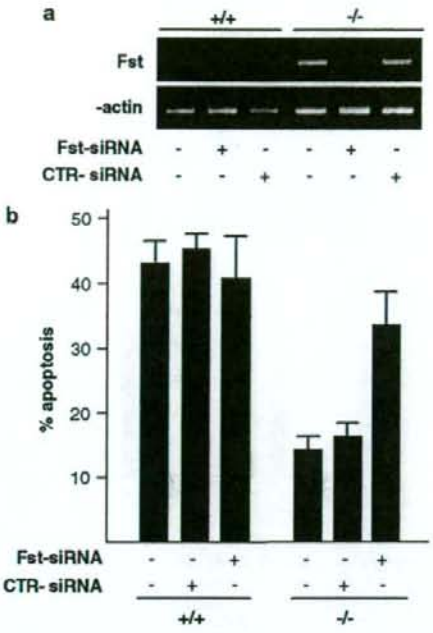

Figure 5 Regulation of apoptosis by endogenous follistatin in *parkin*-deficient cells. (**a**) Primary hepatocytes established from wild-type (+/+) and *parkin*−/− mice were transfected with small-interfering RNA (siRNA) targeting *follistatin*-siRNA (Fst-siRNA) or control siRNA (CTR-siRNA). The expression levels of *follistatin* (Fst, upper panel) or β-*actin* (lower panel) were examined by RT–PCR analyses. (**b**) The percentage of apoptotic cells (mean ± s.d.; $n = 3$) was determined by a trypan blue dye exclusion assay following the culture of Fst-siRNA or control (CTR-siRNA)-transfected mouse primary hepatocytes with 10 μM DOX.

Discussion

The molecular events underlying the development of human HCC are not well understood. However, it is believed that a multistep process of genetic alterations is responsible for hepatocarcinogenesis (Feitelson *et al*., 2002; Laurent-Puig and Zucman-Rossi, 2006). The development and progression of cancers is characterized by inactivation of tumor suppressor genes and by amplification of selected oncogenes (Farazi and DePinho, 2006). Although several transgenic mouse models have been shown to develop liver cancers, the key tumor suppressor molecules involved in hepatocarcinogenesis are unclear. In the present study, we demonstrated for the first time that parkin is important in the regulation of hepatocyte proliferation and apoptosis, and that the loss of parkin expression results in the development of HCC. There is a paucity of data on whether genes associated with Parkinson's disease are important in the biochemical pathways essential for carcinogenesis (West *et al*., 2005). In contrast to epidemiologic studies indicating a negative association between Parkinson's disease and cancer, recent reports suggest that parkin is involved in the development of various human cancers (Cesari *et al*., 2003; Denison *et al*., 2003; Picchio *et al*., 2004; Wang *et al*., 2004). Our present findings, which show that *parkin*−/− mice are susceptible to HCC, provided the evidence suggesting that *parkin* is important as a tumor suppressor gene.

Several other groups independently generated *parkin*−/− mice with various targeted deletions of the *parkin* gene (Goldberg *et al*., 2003; Itier *et al*., 2003; Palacino *et al*., 2004; Von Coelln *et al*., 2004; Perez and Palmiter, 2005). Two groups described exon 3-deleted mice models similar to ours and reported that they had no dopaminergic neuronal loss (Goldberg *et al*., 2003; Palacino *et al*., 2004). A recent report also demonstrated negligible deficits in neurological function, learning or memory in exon 2-deleted models (Perez and Palmiter, 2005). These findings suggest that *parkin*−/− mice do not recapitulate signs central to Parkinsonism. However, all these previous studies focused on phenotypic analyses of the central nervous system. It is thus unclear whether these *parkin*−/− mice developed hepatic